energies

MDPI

Article

Achieving Efficient and Stable Deammonification at LowTemperatures—Experimental and Modeling Studies

Hussein Al-Hazmi [1,*], Xi Lu [1,2], Dominika Grubba [1], Joanna Majtacz [1], Przemysław Kowal [1] and Jacek Mąkinia [1]

[1] Faculty of Civil and Environmental Engineering, Gdansk University of Technology, 11/12 Narutowicza Street, 80-233 Gdańsk, Poland; xilu@pg.edu.pl (X.L.); dominika.grubba@pg.edu.pl (D.G.);joanna.majtacz@pg.edu.pl (J.M.); przkowal@pg.edu.pl (P.K.); jmakinia@pg.edu.pl (J.M.)

[2] Institute of Environmental Science and Engineering, Tongji University, 1239 Siping Road, Shanghai 200092, China

* Correspondence: hussein.hazmi@pg.edu.pl

Abstract: The short-term effects of temperature on deammonification sludge were evaluated in a laboratory-scale sequencing batch reactor (SBR). Mathematical modeling was used for further evaluations of different intermittent aeration strategies for achieving high and stable deammonification performance at decreasing temperatures. As for the biomass cultivated at high temperatures (e.g., 30 °C), a higher temperature dependency (the adjusted Arrhenius coefficient θ for 11–17 °C = 1.71 vs. θ for 17–30 °C = 1.12) on the specific anammox growth rates was found at lower temperatures (11–17 °C) in comparison with higher temperatures (17–30 °C). Further evaluations of recovering the nitrogen removal efficiency at decreasing temperatures with the mathematical model by modifying the intermittent aeration strategies (aeration frequency (F) and the ratio (R) between non-aerated (non-aer) phase and aerated (aer) phase durations) indicated that intermittent aeration with a prolonged non-aerated phase (e.g., R ≥ 4 regardless of F value) would help to maintain high and stable deammonification performance (~80%) at decreasing temperatures (14–22 °C). Extending the non-aerated phases (increasing R) and reducing the frequency (F) of off/on phase changes have a positive effect on increasing energy savings, leading to increasing interest in this method.

Keywords: deammonification; temperature; mathematical modeling; Arrhenius coefficient; intermittent aeration

Citation: Al-Hazmi, H.; Lu, X.; Grubba, D.; Majtacz, J.; Kowal, P.; Mąkinia, J. Achieving Efficient and Stable Deammonification at LowTemperatures—Experimental and Modeling Studies. *Energies* **2021**, *14*, 3961. https://doi.org/10.3390/en14133961

Academic Editor: Carlos Pozo

Received: 12 May 2021
Accepted: 28 June 2021
Published: 1 July 2021

1. Introduction

Numerous deammonification reactors have been operated successfully worldwide in sidestream systems [1–3]. However, mainstream applications of deammonification are still in the "infancy stage" [4]. The authors identified several challenges for the implementation of mainstream deammonification, including low ammonia concentrations and process temperatures (<15 °C).

In order to acclimate deammonification to low temperatures, the operational conditions must be adjusted accordingly so that nitrite-oxidizing bacteria (NOB) suppression continues while the anammox activity is not deteriorated. It is well known that changing the aeration mode from continuous to intermittent has proven to be a beneficial means of improving the deammonification efficiency [5–7]. Other possible modifications comprise reducing the dissolved oxygen (DO) concentration [8,9], extending the hydraulic retention time (HRT) [5], reducing the influent nitrogen (ammonium) loading rate (NLR) [8], increasing the solid retention time (SRT) [10] or adding glycine [11].

Some authors [10,12,13] have suggested that the anammox process starts to fail at 15 °C, resulting in imbalanced nitrogen conversion in deammonification systems. On the other hand, several studies have shown that stable and efficient operation of the

anammox process would still be possible below 15 °C, even though the specific anammox activity (SAA) decreased to 30–40% in comparison with that at the reference temperature of 30 °C [14,15]. In these studies, more pronounced declines in the anammox activity were observed at temperatures below 15 °C. Although the feasibility of the anammox process has been confirmed at such low temperatures (so called "cold anammox") [16,17], the total nitrogen (TN) removal rates decrease dramatically and the stability of the system becomes very sensitive even to small drops in temperature. As a consequence, the TN removal efficiencies may fall at least 10 times when the temperature drops from approximately 30 to 10–12 °C [15].

There have been only a few reports of recovery of the deammonification process at low temperatures by implementing the intermittent aeration strategy [5,8,13,18]. However, intermittent aeration alone would be insufficient for improving the efficiency of the deammonification processes at low temperatures if the lengths of the aeration and non-aeration phases remain unchanged. Extending the non-aerated phase allows anaerobic ammonia-oxidizing bacteria (AAOB) to be more active as they have more time to grow and multiply. These are also conditions that inhibit the development of NOB due to the lower frequency of aerated phases. However, it is important to be careful about the influencing NH_4-N, as excessive concentrations may lead to the inhibition of ammonia-oxidizing bacteria (AOB) and AAOB with free ammonia (FA). Until now, no studies have been carried out that combine the aeration strategy and influent NLR during the gradual reduction in temperature in a granular deammonification sequencing batch reactor (SBR).

Intermittent aeration in the deammonification process provides 60% energy savings compared to conventional biological wastewater treatment processes [19]. This is a particularly important parameter due to the growing interest in sustainable, energy-efficient processes. Extending the non-aerated phases (increasing R) and reducing the frequency (F) of off/on phase changes increases energy efficiency [7].

The aim of this study was to balance the deammonification efficiency with a gradually decreasing temperature (down to 11 °C) by adjusting the intermittent aeration strategy and extending the non-aerated time. The novelty in our experiment lies in changing the durations of the off times of aeration, as previous studies focused on changing aeration from continuous to intermittent or simultaneously changing both the on and off times of intermittent aeration [20–22]. Moreover, we controlled the NLR to avoid FA inhibition at the laboratory scale to determine the lowest temperature at which the process was feasible, while continuously extending the non-aerated time. Advanced microbiological techniques allowed us to evaluate how the microbial population changed with the decreasing temperature. A mathematical model was validated and used to identify the main factors affecting the strategy for recovering efficient nitrogen removal.

2. Materials and Methods

2.1. Origin of the Inoculum Biomass and Laboratory Set-Up

Prior to the present experiments, granular sludge was cultivated for over 300 days in a bench-scale deammonification SBR with a working volume of 10 L. The reactor was inoculated with process biomass from a full-scale sidestream deammonification system in Plettenberg (Germany) and fed with synthetic substrates at a constant temperature of 30 °C [7].

In the present study, the SBR operation was continued for the next 90 days. The reactor was equipped with a thermostatic jacket to maintain set point temperatures. The aeration was controlled with an aeration system consisting of an air pump (Mistral 200, Aqua Medic, Bissendorf, Germany), DO probe (COS22D, Endress+Hauser, Reinach, Switzerland), and an electromagnetic valve. The pH was controlled at 7.5–7.9 with a programmable logic controller (PLC) connected with a pH probe (CPS471D, Endress+Hauser, Reinach, Switzerland) by dosing 1 M solution of NaOH.

2.2. Experimental Procedure

The experiments were carried out at gradually decreasing temperatures: 30, 26, 22, 18, 16, 14, 13, 12, 11 °C. The synthetic feed contained ammonium chloride and trace elements [23,24]. The operating conditions (temperature, NH_4-N loading and aeration settings) are presented in the Supplementary Materials (Table S1). The temperature and NH_4-N loading conditions were decreased step-wise. The intermittent aeration settings (frequency (F) and the ratio (R) between the non-aerated and aerated phase durations at the DO set point = 0.7 mg O_2/L during the aerated phase) were adjusted accordingly to achieve high and stable nitrogen removal performance according to Table S1 and Figure 1. The duration of a single operational cycle of the studied SBR was variable (8–24 h) and the cycle consisted of four phases, i.e., 3 min of sedimentation, 27 min of decantation (4.5 L), 30 min of feeding (4.5 L), 7–23 h of reaction, according to Table S1 and Figure 1. In each phase of the reaction, the aeration time was always 3 min, while the time without aeration ranged between 6 and 57 min. Depending on the duration of the reaction, the frequency of the on/off phase changes varied.

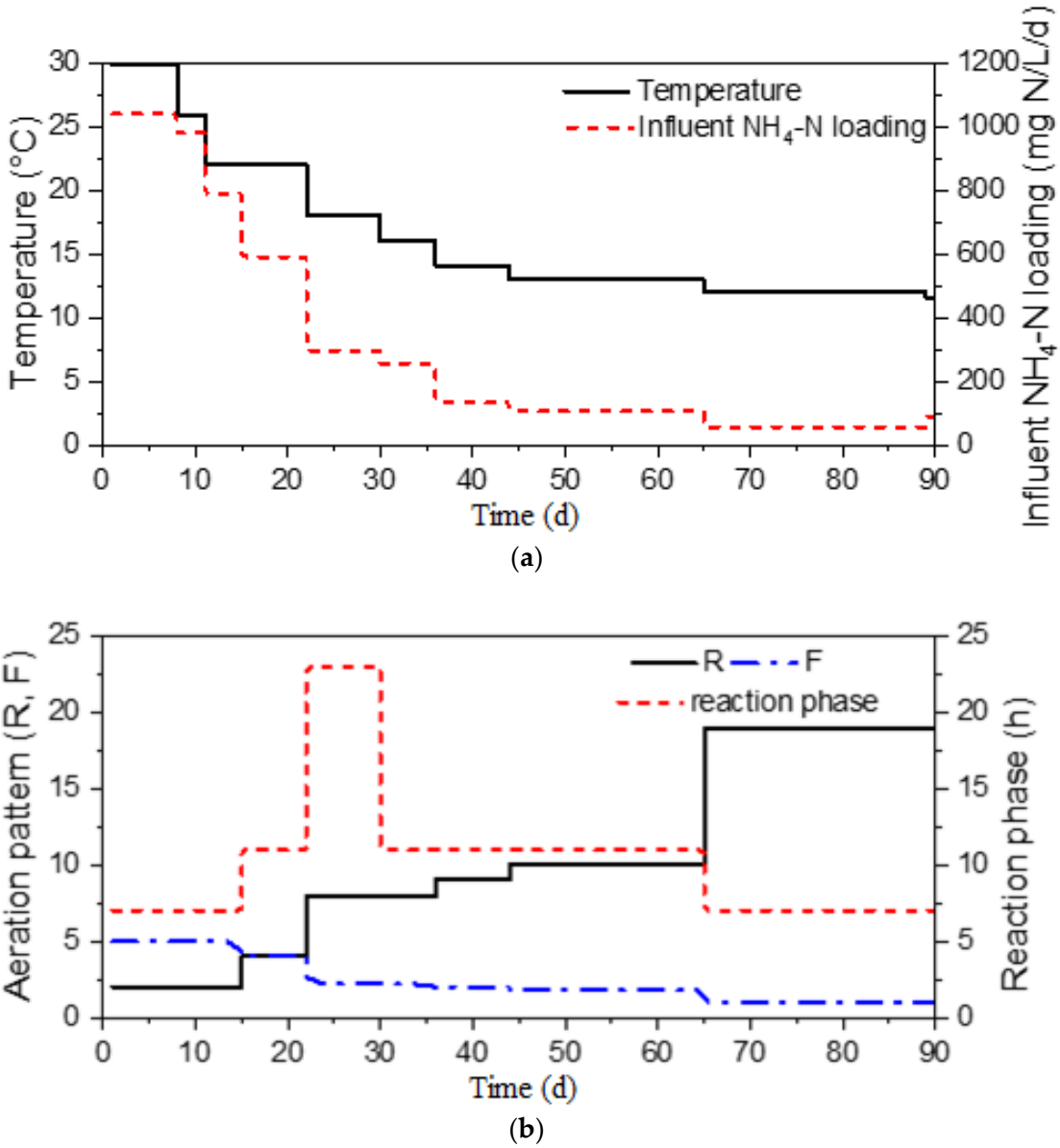

Figure 1. (**a**) Temperature and influent NH_4-N loading; (**b**) the aeration pattern (R and F) and reaction phase duration.

2.3. Analytical Methods

Concentrations of the inorganic N forms (NH_4–N, NO_3–N, NO_2–N) were determined in the filtered mixed liquor during the course of the batch experiments. Two 50 mL mixed liquor samples were withdrawn during this experimental period to determine the mixed liquor suspended solids (MLSS) concentration and its volatile fraction (MLVSS) according to Standard Methods (APHA, 2005). The measurements were carried out using cuvette tests (Hach Lange GmbH, Berlin, Germany) in DR3900 Benchtop Spectrophotometer (Hach Lange GmbH Berlin, Germany). The specific ammonium utilization rate (AUR) and nitrate production rate (NPR) were determined based on the maximum slope of NH_4-N consumption and NO_3-N production in the reaction phase. FA values were calculated based on Anthonisen et al. [25].

2.4. Organization of the Simulation Study

2.4.1. Mathematical and Simulation Model

The Activated Sludge Model no. 1 (ASM1) was extended with partial nitritation/denitritation and anammox processes, as well as the N_2O production and emission pathways with the same model parameters adopted from Al-Hazmi et al. [7] and Lu et al. [26]. The model was implemented in the simulation platform GPS-X 8.0 (Hydromantis, Hamilton, ON, Canada). The simulation model layout consisted of a 10L SBR, an influent object, a timer controller and a modeling toolbox. The reactor was operated under different conditions, as summarized in Table S1. The timer controller allowed us to simulate the actual intermittent aeration pattern by setting the aeration cycle time, the aerated phase duration in one cycle and the DO set point during the aerated phase. The DO set point was achieved by manipulating the field oxygen mass transfer coefficient (KLa) with the integrated PI controller (sampling time—20 s, proportional gain—500, integral time—0.0001 d). The pH was calibrated based on the model developed by Vavilin et al. [27] in the modeling toolbox. In order to reduce model uncertainty, the initial microbial composition for model input was based on metagenomics analysis.

2.4.2. Estimation of the Temperature Correction Factors and Application in the Simulation

The temperature effects on the maximum specific growth rates of the functional microorganisms were evaluated using the Arrhenius equation (Equation (1)):

$$\mu_{max,T} = \mu_{max,T_0} \cdot \theta^{(T-T_0)} \quad (1)$$

where T and T_0 are the actual and reference temperatures, respectively, μ_{max,T_0} is the maximum specific growth rate at T_0, and θ is the temperature correction factor (Arrhenius coefficient).

The equation fundamentally considers energy partitioning at a steady-state temperature, while the biokinetics are predominantly driven by fluctuations near equilibrium [28].

The temperature activation energy was determined based on the natural logarithm of the Arrhenius equation (Equation (2)):

$$\ln(\mu_{max,T}) = \ln(A) - \frac{E_a}{8.314 \cdot T} \quad (2)$$

where E_a is the apparent activation energy (kJ·mol^{-1}); A is the frequency factor for the reaction; 8.314 is the universal gas constant (J/(mol·K)) and T is the temperature in K.

Considering that a high cell density limits substrate availability especially under low NH_4-N loading conditions, the Arrhenius coefficients on the maximum specific growth rates of AOB and anammox bacteria were scaled against the cell density and applied in the simulation. The predicted NH_4-N, NO_2-N, NO_3-N, N_2O in the liquid were compared with the measured data to fulfil the goodness-of-fit criterion (Pearson's r > 0.9). The conversion pathways of the N equivalents were visualized in a Sankey graph and the differences between different temperatures were visualized in a heatmap.

2.4.3. Model-Based Analysis of the Aeration Strategies for Highly Efficient and Stable Deammonification

Different intermittent aeration strategies were analyzed within the temperature range 11–30 °C. The operating parameters of interest, i.e., F and R, were manipulated within the range 1–5 (interval of 1) and 1–20 (interval of 5) at DO set point = 0.7 mg O_2/L. Altogether, 250 automatic simulations were carried out by executing Python 3.7 scripts within the GPS-X 8.0 interface. The 2D response contour plots of the operational parameters on the AOB activity and NOB activity were generated in MATLAB R2019b (The MathWorks, Inc., 3 Apple Hill Dr in Natick, Massachusetts, USA).

2.5. Microbiological Analyses

2.5.1. Sampling and DNA Extraction

For metagenomic analysis, samples of biomass were collected on the following experimental days: 1, 23, 33, 55, 88, 99. DNA extraction from 100 mg of the biomass samples was performed in duplicate by the use of Fast DNA™ Spin Kit for Soil (MP Biomedicals, USA), in accordance with the manufacturer's protocol.

2.5.2. High-Throughput Illumina 16S rRNA Gene Sequencing and Bioinformatics Analysis

After extraction, genomic DNA was subjected to quality analysis with spectrophotometry at 260/280 wavelength ratio. Subsequently, standardization of the DNA concentrations was performed in order to obtain 100 ng/µL. Based on the DNA matrix, gene libraries of 16S rRNA gene V3-V4 region were constructed with 341F and 785R primer set, as proposed by Klindworth et al. [28]. MiSeq sequencer by Illumina (Illumina, Inc., Hayward, CA 94545 USA) was applied to carry out sequencing reactions, performed by an external service supplier. Obtained DNA sequences were processed with tools available at Usegalaxy server (https://usegalaxy.org (accessed on 18 February 2021)), by initial paired-end read joining (with FASTQ joiner), followed up by adapter and primer trimming, finalized with quality control (DNA sequences at cut-off value $\leq$ 20 and length $\leq$ 100 bp were excluded) with FASTQ/A algorithm [29]. The last step of data quality control involved chimera presence detection performed with the USEARCH 6.0 online tool available at http//fungene.cmeplatform (accessed on 1 July 2021).

After quality analysis, DNA sequence reads were subjected to the classification step with the use of the Silva NGS platform available at http://www.arb-silva.de (accessed on 1 July 2021) at 90% species similarity and clustered into OTUs (operational taxonomic units) at 97%.

In order to determine the genetic distance between microbial communities during the following experimental phases, an ANOVA test, followed by a post hoc Tukey–Kramer test at 0.95 significance, was conducted using the Statistical Analysis of Metagenomic Profiles (STAMP v. 2.1.3) [30] tool. The same software was implemented to visualize the obtained results in the form of a heatmap by application of the average neighbor (UPGMA) algorithm and a principal component analysis (PCA) plot.

2.5.3. Biodiversity and Correlation Calculations

Biodiversity of the samples was assessed based on the calculation of the Shannon (H) and Simpson diversity (D) indices, calculated with the following formulas (Equations (3) and (4)):

$$H = -\sum_{i=1}^{R} pi \ln pi \quad (3)$$

$$D = 1/\sum_{i=1}^{R} p^2 \quad (4)$$

where pi is the ratio between the number of DNA sequences assigned to the particularity genus to the total number of reads obtained from the sample.

Correlation coefficients reflecting dependencies between individual taxa abundance and biodiversity index values against the operational parameters modified during the

following experimental stages (temperature, NH_4-N load and R ratio) were calculated by the following formula (Equation (5)):

$$r_{XY} = \frac{\sum \left(x_i - \bar{x}\right)\left(y_i - \bar{y}\right)}{\sqrt{\sum \left(x_i - \bar{x}\right)^2 \sum \left(y_i - \bar{y}\right)^2}} \quad (5)$$

where: r_{xy}—correlation coefficient of the linear relationship between the variables x and y; x_i—the values of the x variable in a sample; $\bar{x}$—the mean of the values of the x variable; y_i—the values of the y variable in a sample, $\bar{y}$—the mean of the values of the y variable.

3. Results and Discussion

3.1. Process Performance at Decreasing Temperatures

A short deterioration in the deammonification process was observed on day 11 of the experiment (Figure 2). This was the effect of the temperature drop from 30 °C to 22 °C, which caused a sharp drop in the apparent TN removal efficiency (TNRE = 76–36%) due to around half of the AOB and AAOB activity (AUR = 13–7.9 mg N/g VSS/h) and relatively increased NOB activity (NPR/AUR = 0.07–0.10). At the optimal temperatures of 30–40 °C, the AAOB doubling time was 7–14 days [31,32]. At lower temperatures, the AAOB doubling time could be up to 10 times longer [33]. The increased NO_2-N concentrations also confirmed the increased activity of AOB compared to AAOB [12]. The accumulation of NO_2-N is a common symptom of decreased AAOB activity [12,34,35].

To improve the efficiency of the deammonification process, the time of the non-aerated phase was extended from 6 to 12 min and the concentration of the influent NH_4-N load was lowered from 790 mg N/dm^3/d to 590 mg N/dm^3/d on day 15. This resulted in both reduced NO_2-N and NO_3-N production and improved NH_4-N removal efficiency. This efficiency increased from 60% to 88%, whereas the apparent TN removal efficiency returned to 71% due to higher NOB suppression (NPR/AUR = 0.06). However, the actual TN removal efficiency was still low (NNRE = 44%), which was attributed to lower AOB and AAOB activities at 22 °C (AUR = 6.2 mg N/g VSS/h).

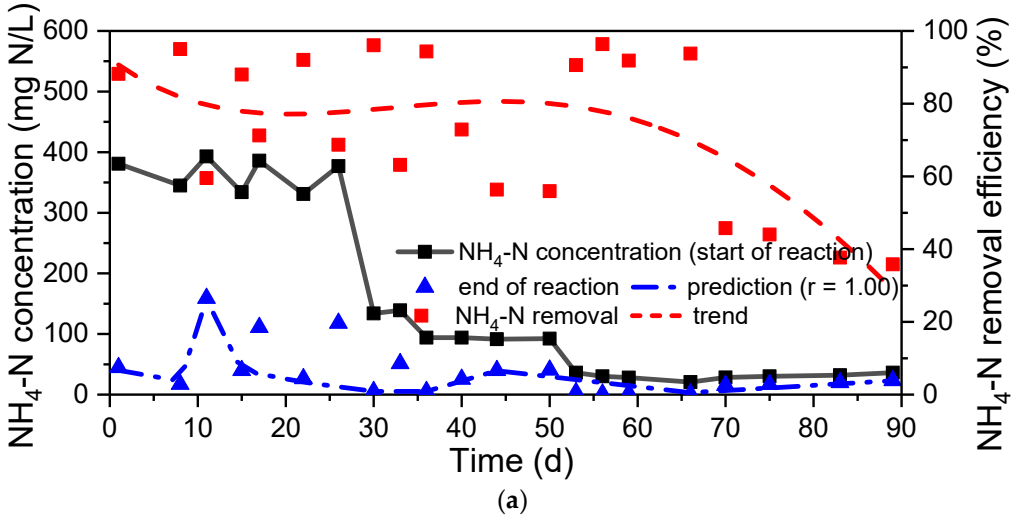

(**a**)

Figure 2. *Cont.*

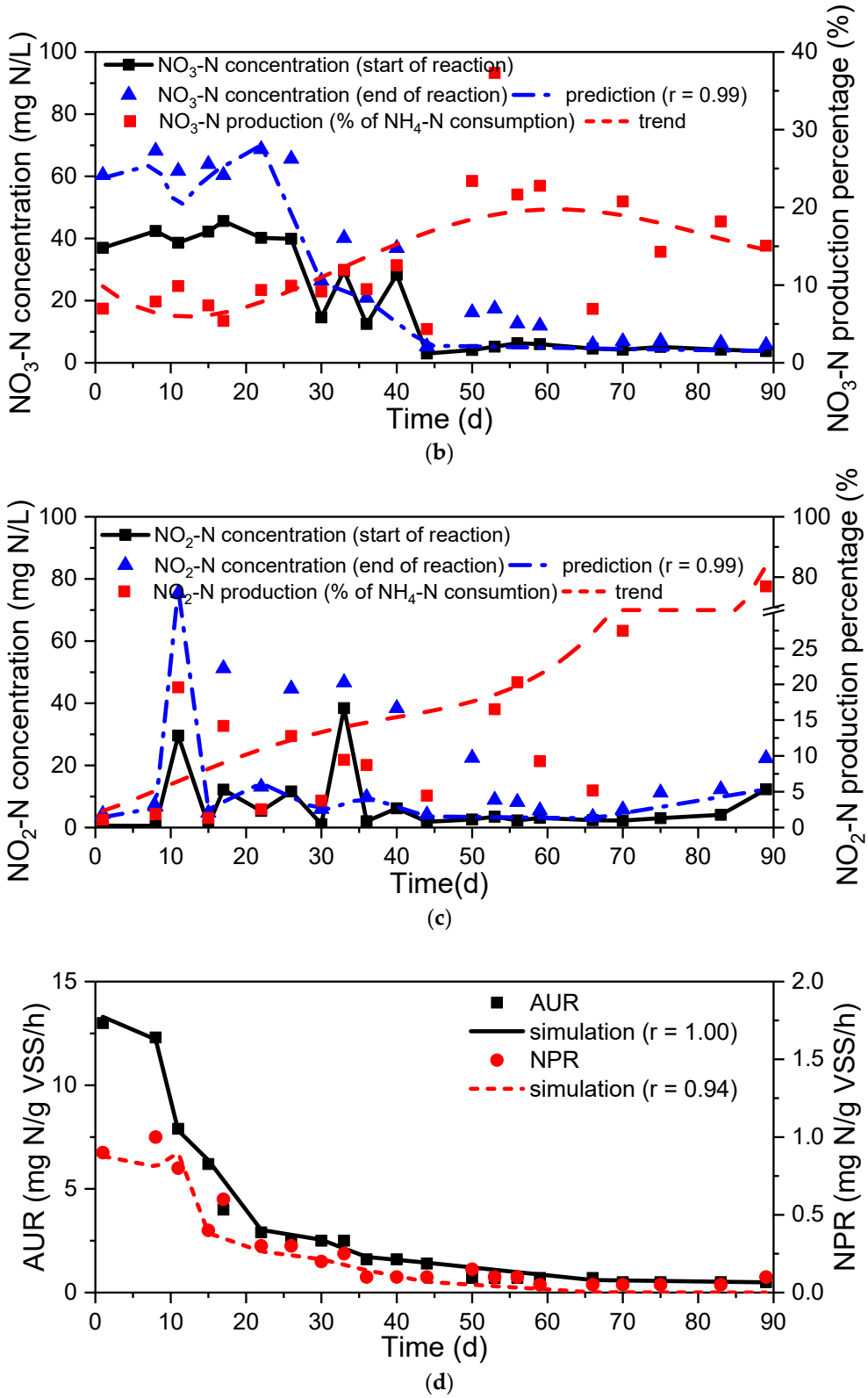

Figure 2. (**a**) Measured (scatters) and predicted (dashed (dotted) line) NH_4-N concentrations at the beginning and end of the reaction phase, and NH_4-N removal efficiency; (**b**) measured (scatters) and predicted (dashed (dotted) line) NO_3-N concentrations at the beginning and end of the reaction phase, and NO_3-N production (% of NH_4-N consumption); (**c**) measured (scatters) and predicted (dashed (dotted) line) NO_2-N concentrations at the beginning and end of the reaction phase, and NO_2-N production (% of NH_4-N consumption); (**d**) measured (scatters) and predicted (dashed line) AUR and NPR.

Akaboci et al. [13] found that NOB were able to acclimate to the conditions of intermittent aeration. This presents a challenge for carrying out the deammonification process with alternating aerobic and anaerobic phases, and low temperatures increase the difficulty of NOB inhibition [10,12,13]. Moreover, it risks losing the activity and makes it difficult to resume the process when the temperature rises again, as reported by Lackner et al. [36].

High concentrations of NH_4-N can inhibit the anammox process [36]. In the case of a gradual decrease in temperature, excessive concentrations of NH_4-N may completely halt the deammonification process. There are reports indicating that the gradual acclimation of anammox bacteria to temperatures below 15 °C is possible [37–39]. However, the acclimation period should be long enough to compensate for the decreasing growth rates of anammox bacteria [38,40]. Isanta et al. [41] reported that controlling the concentration of DO together with the concentration of NH_4-N enabled stable partial nitritation at low temperatures.

However, when the temperature was only 11 °C, the apparent TN removal efficiency decreased to 2%, and the system completely lost its activity (NNRE = 2%).

Feng et al. [37] noted that FA and FNA can reduce the activity of both AOB and NOB, but with a greater effect on NOB. At high levels of FA, NOB were inhibited without adversely affecting the growth of AOB (Figure 3). The implementation of such a strategy was successful in sidestream systems [4]. However, inhibiting FA is more difficult in mainstream conditions with low concentrations of FA, low temperature and continuous flow. The FA concentrations were 8.6–20.9 mg N/dm^3 at 30 °C and 0.2–0.5 mg N/dm^3 at 11 °C (Table 1). In Figure 3, it can be seen that the temperature decreased with the decreased inhibition of NOB. Inhibition of nitration usually occurs after exceeding the FA concentration limit of 0.1–1 mg N/dm^3 [25].

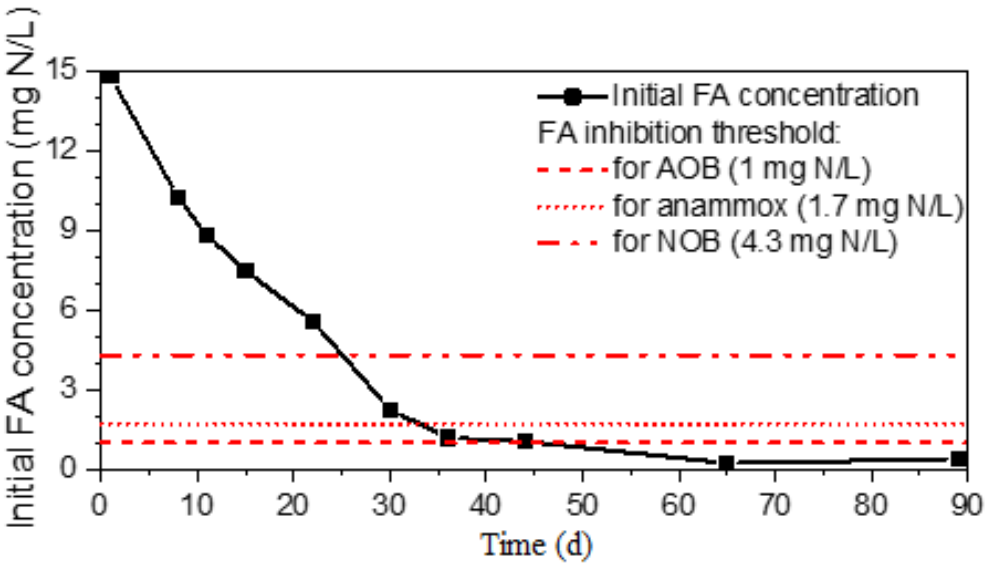

Figure 3. Initial FA concentration and FA thresholds for AOB [25], NOB [41] and AAOB [42].

3.2. Mathematical Modeling

3.2.1. Setting the Initial Biomass Composition for Simulations

The initial biomass compositions (XHET, XAOB, XNOB, XAMX, XS, XU, XEPS) for 30, 26, 22–16, 14–13, 12, 11 °C were (i) 47%, 9%, 0.12%, 2.4%, 38%, 3.3%; (ii) 32%, 21%, 0.09%, 2.1%, 41%, 3.6%; (iii) 33%, 22%, 0.08%, 5.5%, 36%, 3.2%; (iv) 28%, 21%, 0.06%, 6.1%, 41%, 3.6%; (v) 32%, 5.6%, 0.14%, 7.5%, 50%, 4.4%; (vi) 34%, 2.9%, 0.09%, 3.5%, 55%, 4.8%.

Table 1. The measured AURs and NPRs during the study period.

Day	Temperature (°C)	Initial Bulk FA at pH = 7.5–7.9 (mg N/L)	AUR (mg N/g VSS/h)	NPR (mg N/g VSS/h)	NPR/AUR
1	30	8.6–20.9	13	0.9	0.07
8	26	6.6–16.2	12.3	1	0.08
11	22	3.8–9.3	7.9	0.8	0.10
15	22	4.2–10.4	6.2	0.4	0.06
17	18	4.2–10.4	4.0	0.6	0.15
22	18	3.0–7.5	2.9	0.3	0.10
26	16	3.0–7.5	2.5	0.3	0.12
30	16	1.1–2.8	2.5	0.2	0.08
33	14	1.1–2.8	2.5	0.25	0.10
36	14	0.5–1.3	1.6	0.1	0.06
40	13	0.5–1.3	1.6	0.1	0.06
44	13	0.4–1.0	1.4	0.1	0.07
50	12	0.4–1.0	0.7	0.15	0.21
53	12	0.4–1.0	0.7	0.1	0.14
56	12	0.4–1.0	0.7	0.1	0.14
59	12	0.4–1.0	0.7	0.05	0.07
66	12	0.1–0.3	0.7	0.05	0.07
70	11	0.1–0.3	0.5	0.05	0.10
75	11	0.1–0.3	0.5	0.05	0.10
83	11	0.1–0.3	0.5	0.05	0.10
89	11	0.2–0.5	0.5	0.1	0.20

3.2.2. Temperature Effects on Bacterial Growth

As the temperature decreased from 30 to 11 °C, the abundances of functional microorganisms, especially AOB and AAOB, varied in the range of 3–22% and 2–7.5%, along with a general increase in the total biomass concentration (3.6–4.9 g VSS/L). After applying the Monod functions, the decrease in the AOB and AAOB growth rates could be attributed to two major causes, i.e., the lower microbial activities at decreasing temperatures and the lower substrate availability.

The Arrhenius coefficient (θ) for AOB was 1.12. Two different θ values, i.e., 1.63 and 1.11, were applied for AAOB in the temperature ranges 11–16 °C and 16–30 °C (Figure 4a). The anammox temperature activation energies (E_a) were 507 and 78.7 kJ·mol-1, respectively (Figure 4b). The predicted N compounds (NH_4-N, NO_2-N, NO_3-N, N_2O in the liquid phase) were compared with the measured data, and good agreement was found (Figure 2, Pearson's r close to 1).

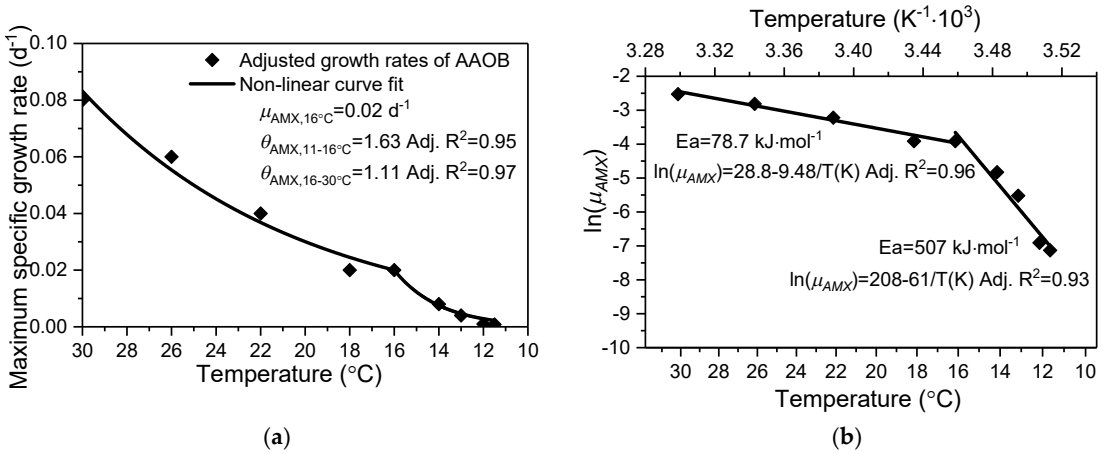

(**a**) (**b**)

Figure 4. The temperature effects on the specific anammox growth rates in the studied SBR described by the Arrhenius equations in two temperature ranges (**a**), and estimation of the activation energy (E_a) in the two temperature ranges (**b**).

The E_a values could vary from 6 to 437 kJ/mol in terms of different temperature ranges, different reactor configurations, different genera of anammox and under different operational conditions [10,11,15,43–45]. In general, lower E_a values were found at higher investigated temperature ranges, i.e., 6–239 kJ/mol for T = 15–40 °C vs. 93–437 kJ/mol for T = 6–28 °C. In the present study, the E_a values, estimated for the lower temperature range, were slightly higher than the reported values. This may indicate higher temperature sensitivity and the difficulty of achieving efficient nitrogen removal under low temperatures.

3.2.3. Temperature Effects on the N Conversion Pathways

N conversion pathways were investigated with the validated model at decreasing temperatures (Figure 4a). When the temperature decreased from 30 to 11 °C, the system managed to recover efficient and stable deammonification performance twice when three failures were encountered, as described below.

The first failure occurred on day 11. When the temperature dropped from 30 to 22 °C, the first decrease in the NH_4-N removal efficiency (<60%) was mainly attributed to the sharp decrease in the anammox activity (Figure 4a). Prolonging the non-aerated phase duration (R value from 2 to 4) and reducing the influent NH_4-N loading (from 790 to 590 mg N/(L·d)) could protect AAOB from the inhibitory effects of DO and FA (threshold of 1.7 mg N/L, Figure 3) and effectively recover the NH_4-N removal efficiency back to 90%.

The first recovery occurred on day 15 at a moderate temperature (22 °C). NH_4-N conversion and nitrogen removal were mainly attributed to AOB and anammox activities, respectively (Figure 5b). A substantial amount of N_2O was produced in comparison with the removed nitrogen load, which was mainly attributed to the autotrophic denitrification (AD) pathway mediated by AOB. NO_2-N accumulation was affected by the balance between NO_2-N production by AOB and NO_2-N consumption by AD (63%), AAOB (27%) and NOB (10%), whereas heterotrophic denitrification played a negligible role at decreasing temperatures. NO_3-N accumulation in the system was attributed to the NOB activity (70%) during the aerated phase and AAOB (30%) during the non-aerated phase.

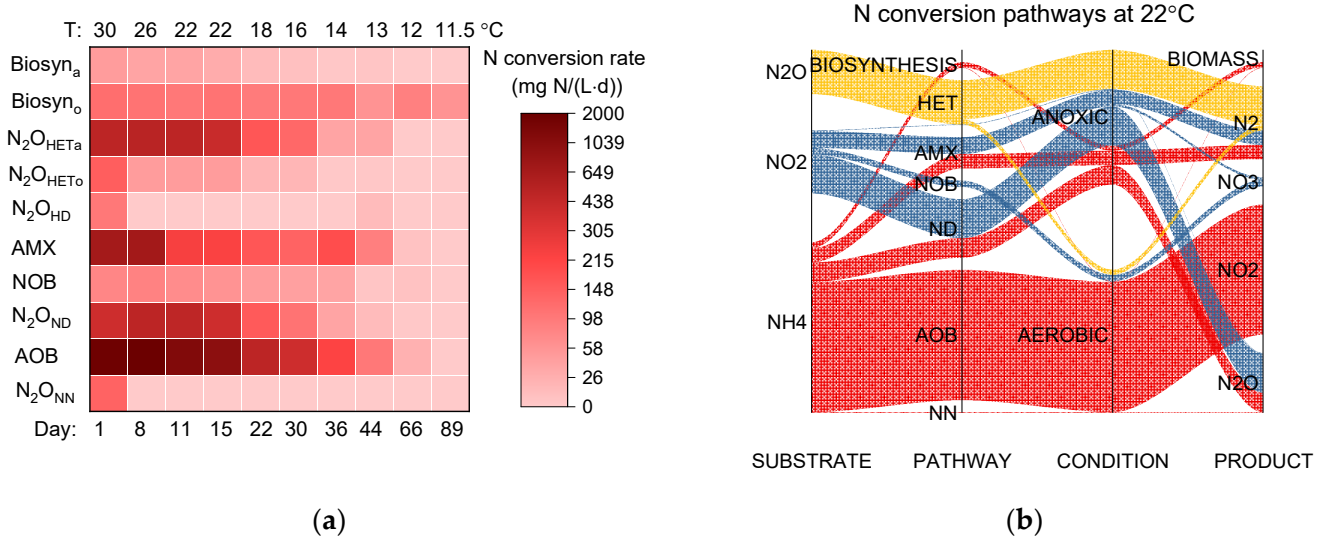

Figure 5. Significant N conversion pathways in the studied system: NH_4^+ oxidation to NO_2^- by AOB (AOB), NH_4^+ and NO_2^- consumption by anammox (AMX), NO_2^- oxidation to NO_3^- by NOB (NOB), N_2O production by heterotrophs (N_2O_{HD}), N_2O production by nitrifier denitrification (N_2O_{NN}), N_2O production by nitrifier denitrification (N_2O_{ND}), N_2O consumption by heterotrophs under anoxic and aerobic conditions (N_2O_{HETa}, N_2O_{HETo}), biosynthesis using NH_4^+ to grow biomass under anoxic and aerobic conditions ($Biosyn_a$,$BioSyn_o$). (**a**) Heatmap of the N conversion pathways in the temperature range 30–11 °C, in which the darker color means higher N conversion rate; (**b**) Sankey graph of the pathway contribution of the N equivalents at 22 °C after recovery, which shows the balance between the major N compounds and their conversions.

The second failure occurred on day 44. When the temperature dropped from 16 to 13 °C, the second decrease in the NH_4-N removal efficiency (<60%) was mainly attributed to the sharp decrease in the AOB activity. From day 36 to 44, the AOB and anammox activities were comparable to that of anammox in the temperature range 13–14 °C, not only due to the inhibitory effect of low temperatures, but also attributed to the prolonged non-aerated phase (detailed in Section 3.3). Decreasing the influent NH_4-N loading further (from 130 to 110 mg N/(L·d)) protected AOB from FA inhibition (threshold of 1 mg N/L, Figure 2). A combined strategy of increasing the non-aerated phase (R value from 9 to 10) and decreasing the NH_4-N loading could recover the NH_4-N removal efficiency back to 90%.

The final failure occurred on day 89. When the temperature decreased below 12 °C, the system lost both AOB and AAOB activities (Figure 5a).

3.2.4. Model-Based Analysis of the Aeration Strategies for Efficient and Stable Deammonification Performance at Decreasing Temperatures

At decreasing temperatures, the increasing R could slow down the decrease in the AUR and maintain the relatively low NPR/AUR. The frequency F had no effect on AUR or NPR/AUR at low temperatures. However, low frequency F is desirable at high temperatures. The modeling results indicate that in order to maintain the deammonification process at low temperatures, the off/on ratio (R) should therefore be increased to obtain the lowest NPR/AUR ratio (Figure 6).

3.3. Microbial Community Structure Adaptation to the Experimental Conditions

3.3.1. Shannon's and Simpson's Diversity

The diversity of the microbial community, expressed as Shannon's and Simpson's diversity indices, showed a general increasing trend during the entire study period (Table 2).

Table 2. Shifts in Shannon's and Simpson's diversity index values during experiment with correlations to modifications of temperature, NH_4-N load and R value.

Sample	Initial 30 °C	Day 10 26 °C	D21 22 °C	D39 14 °C	D68 12 °C	D87 11 °C	Temp.	R	Load
Shannon's diversity (H)	3.54	3.56	3.55	3.66	3.83	4.05	−0.82	0.90	−0.76
Simpson's diversity (D)	17.43	15.05	14.14	15.86	25.77	27.79	−0.69	0.88	−0.64

Shannon's diversity (H), which is used to estimate overall biodiversity, was stable at the temperature range of 22 °C–30 °C, while Simpson's diversity (D) gradually decreased. After switching to 14 °C, both indices started to elevate their values and reached the maximum during the last experimental phase. Simpson's diversity (D) is especially vulnerable to the occurrence of some predominant microbial groups, which suggests that the initial experimental conditions favored some selected bacterial groups, while during the terminal stage, the community was composed of more versatile and evenly distributed taxa. The biodiversity reflected a strong negative correlation in terms of temperature and NH_4-N load, while a positive correlation was observed in relation to the extended non-aerated phase.

3.3.2. Differences in the Genetic Distance between Microbial Community Composition in Samples from the Distinct Experimental Stages

Results of the PCA analysis showed the directed adaptation of the microbial community structure over the entire study period, along with the temperature decrease (Figure 7).

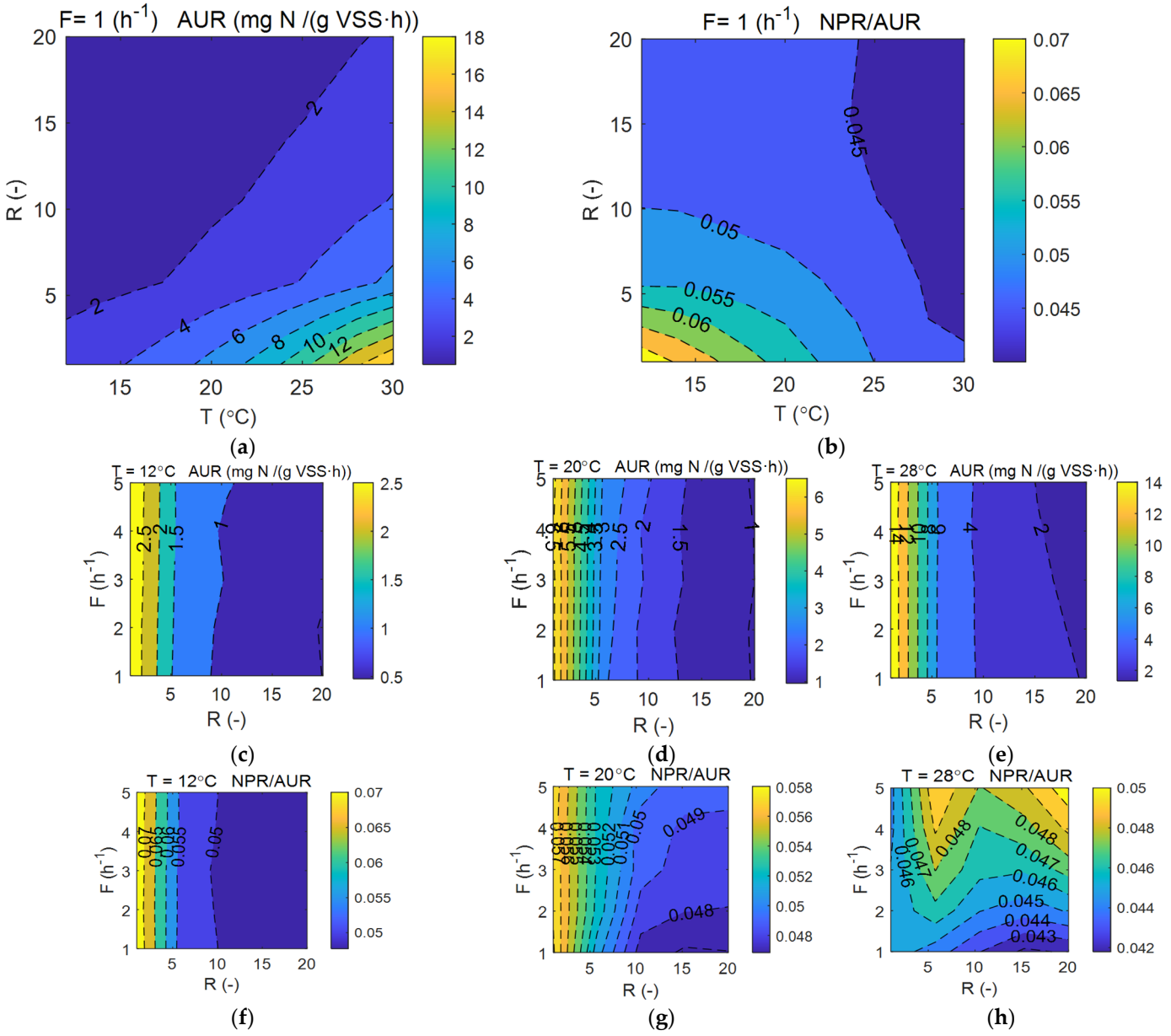

Figure 6. 2D response contour plots for the operational parameters of temperature and aeration strategy (F frequency, R ratio) on the AUR and NPR: the impact of the off/on ratio (R) and temperature on (**a**) AUR, (**b**) NPR/AUR at the fixed frequency (F) = 1 h^{-1}, the impact of frequency (F) and off/on ratio (R) ratio on (**c**–**e**) AUR and (**f**–**h**) NPR/AUR at different temperatures (12, 20, 28 °C).

A notable reorganization of the bacterial consortium composition was observed after the temperature changed from 30 °C to 26 °C, which corresponded to the long distance between the points on the PCA plot. After this stage, the bacterial community showed a relatively stable structure within the temperature decrease from 26 °C to 14 °C (data points formed a compact cluster, as seen in Figure 7) and again was subjected to the sharp reorganization after the process temperature was lowered to 12 °C. The temperature decreases to 11 °C stimulated the selection processes; however, the microbial community's structure was more closely related to the samples from the temperature range of 14–26 °C rather than 12 °C. This suggested that it tended to restore its optimal composition, not strictly as a response to the applied temperature but rather in terms of restoration of the functional properties and interspecies interactions.

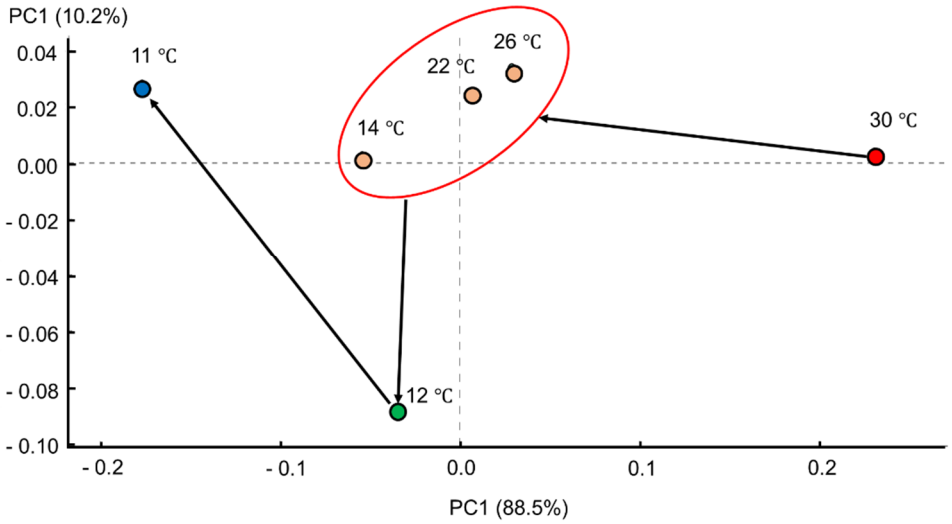

Figure 7. PCA plot of the differences in the genetic distance between the microbial community composition in the samples from the distinct experimental stages, validated with the ANOVA test using the STAMP software ($p < 0.05$).

3.3.3. Changes in Composition of the Microbial Community

At the beginning of the study, the microbial community was predominated by heterotrophic members of the *Anaerolineae* class from the *Chloroflexi* phylum, which accounted for 33.5% of the total bacterial community. Representatives of *Chloroflexi* reduced sharply their abundance, which was around three times lower (8.8%) at the end of the study (Table 3) and was the most pronounced component of the microbial community (Figure 8). The predominant role of *Chloroflexi* was overtaken by a wide range of *Proteobacteria* phylum members, according to the Supplementary Materials (Figure S1).

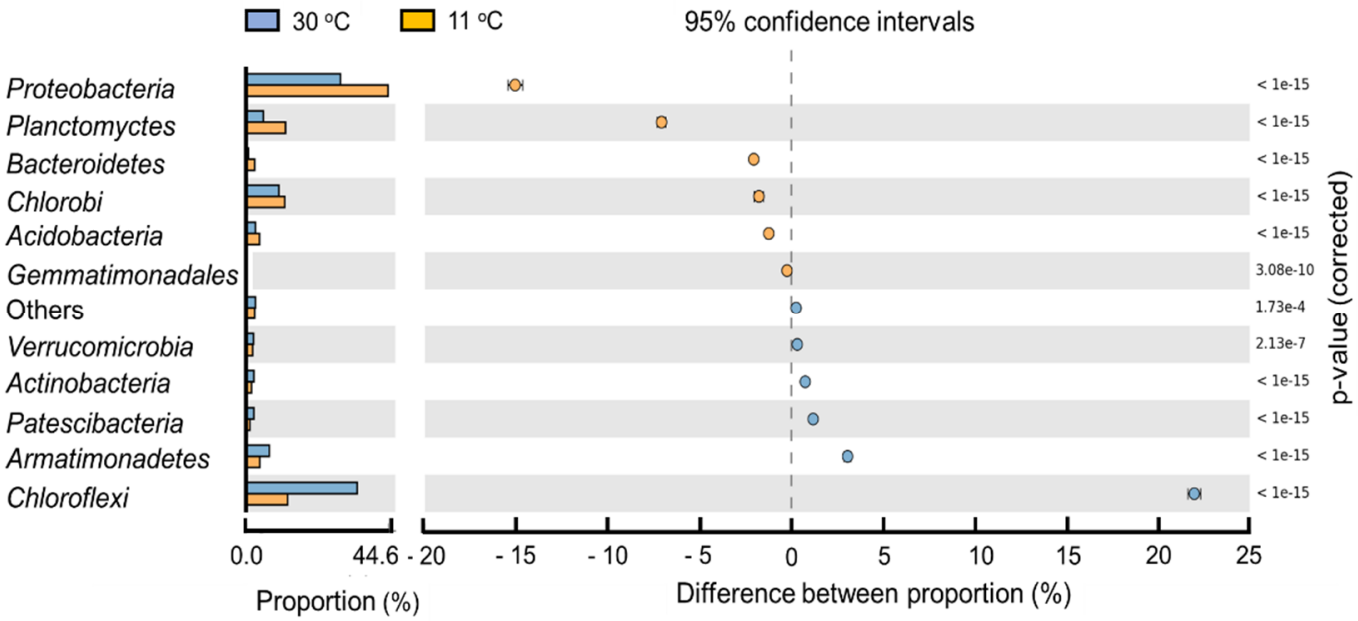

Figure 8. Statistical differences at 95% confidence intervals of the bacterial phyla abundances in the initial (at 30 °C blue) and terminal samples (at 11 °C orange).

Table 3. Percentage of the specified bacterial taxa in the total microbial community with the correlation matrix reflecting dependencies between individual taxa abundance against temperature, NH_4-N load and R ratio. The colors indicate correlation direction and strength (red and orange—strong and moderate negative; dark and light green—strong and moderate positive, respectively).

Physiological Function in Biomass	Affiliation at Specified Taxonomic Level	Abundance of the Specific Bacterial Group in Total Bacterial Community (%)						Correlation			Growth Trend
		D0 30 °C	D10 26 °C	D21 22 °C	D39 14 °C	D68 12 °C	D87 11 °C	Temp	R	Load	
AOB	*Proteobacteria>Betaproteobacteria>Nitrosomonadales>**Nitrosomonas***	9.0	20.6	22.1	20.8	5.6	2.9	0.4	−0.6	0.4	▼▲
NOB	*Nitrospirae>Nitrospira>Nitrospirales>Nitrospiraceae>**Nitrospira***	0.12	0.09	0.08	0.06	0.14	0.09	0.1	0.2	0.1	▼▲
Anammox	*Planctomycetes>Planctomycetacia>Planctomycetales>Planctomycetacea>**Candidatus*Brocadia**	2.4	2.1	5.5	6.1	7.5	3.5	−0.7	0.6	−0.8	▲
HET/Sulphur	*Proteobacteria>Betaproteobacteria> Burkholderiales> Burkholderiaceae> **Limnobacter***	1.7	2.6	2.6	2.8	4.1	3.1	−0.8	0.9	−0.8	▲
	*Proteobacteria>Deltaproteobacteria> **Desulfovibrionales***	4.3	7.5	5.5	5.4	6.6	5.5	−0.2	0.2	0.0	▼▲
	*Chlorobi>Ignavibacteria>**Ignavibacteriales***	1.2	1.9	1.8	1.5	1.8	2.2	−0.6	0.7	−0.5	▼▲
HET *	*Acidobacteria>Solibacteres>Solibacterales>Solibacteraceae>**Bryobacter***	1.0	1.3	1.6	1.2	1.6	0.7	0.0	0.0	0.0	▼▲
	*Armatimonadetes>Fimbriimonadia>Fimbriimonadales**>Fimbriimonadaceae***	7.0	4.5	2.9	2.7	4.0	2.1	0.8	−0.6	0.7	▼
	*Chloroflexi>**Anaerolineae***	33.5	21.0	20.8	15.6	11.7	8.8	0.9	−0.9	0.9	▼
	*Proteobacteria>Betaproteobacteria> Burkholderiales>Comamonadaceae> **Comamonas***	0.9	0.8	1.8	2.9	6.1	4.1	−0.9	0.9	−0.9	▲
	*Proteobacteria>Betaproteobacteriales> Rhodocyclales>Rhodocyclaceae>**Denitratisoma***	1.1	2.8	3.9	4.4	6.9	13.1	−0.8	0.9	−0.7	▲
	*Proteobacteria>Gammaproteobacteria> Pseudomonadales> Pseudomonadaceae>**Pseudomonas***	0.0	0.1	0.1	0.1	0.0	4.4	−0.5	0.6	−0.4	▼▲
	*Proteobacteria>Gammaproteobacteria> Xanthomonadales> Rhodanobacteraceae>**Dokdonella***	2.5	1.5	1.4	1.1	1.6	1.2	0.7	−0.5	0.7	▼

* In terms of the heterotrophic bacteria (HET), representatives of the most numerous genera, showing percentages higher than 1% in at least one sample, were shown.

Among *Proteobacteria*, when the temperature decreased from 30 °C to 14 °C, the highest increase in abundance was observed for the *Nitrosomonas* genus, which doubled their share in the microbial community (increase from 9.0% to approx. 21%). After reaching 12 °C, their abundance sharply decreased to 5.6% and continued to drop in the terminal stage of the study (2.9%). The correlation matrix showed that the non-aerated phase duration was the main factor responsible for the reduction in the *Nitrosomonas* abundance (Table 3).

Typical NOB were represented by the *Nitrospira* genus from the *Nitrospirae* phylum, which showed stable abundance at a low level (average 0.1%). This suggests that NO_3-N production was contributed by the high activity of *Nitrospira*.

The DNA sequences, specific for the bacteria related to the *Planctomycetes* phylum, accounted for at least of 4.5% of the total bacterial community in all the samples. The dominant representatives of *Planctomycetes* were anammox bacteria from the Candidatus Brocadia genus. The abundance of *Candidatus* Brocadia in the initial sample was 2.5% and almost doubled after 21 days. The maximum abundance (7.5%) was reached on day 68 at 12 °C, and then drastically reduced after a prolonged low temperature was applied.

Lotti et al. [14] found that the AAOB affiliated with the Brocadia species were able to survive and grow at 5–6 °C and thus outcompeted *Candidatus* Kuenenia under low temperatures. In the present study, *Candidatus* Brocadia demonstrated effective cultivation despite the process temperature being decreased to 12 °C and the NH_4-N loading rate being lowered. The increased abundance of *Candidatus* Brocadia proved that the selected conditions, including prolongation of the non-aerated phase, were optimal to operate the deammonification system.

Microbial analysis conducted by Wu et al. [17] with high-throughput 16S rRNA gene sequencing revealed that representatives of *Candidatus* Brocadia sinica displayed relatively high abundances (13% of the total bacterial community) in a system operated at 13 ± 2 °C, which ensured a rapid start-up of the cold anammox process and allowed them to successfully operate the system for 90 days.

3.4. Energetic Aspects of the Application of the Deammonification Process

The use of the deammonification process for wastewater treatment is justified in terms of energy. Compared to traditional technology using nitrification and denitrification processes, deammonification reduces aeration costs by around 60–65% [46], does not require an additional carbon source and reduces excess sludge [37] and carbon dioxide emissions by 90%, as well as reducing nitrous oxide [47–49].

Our low temperature research also has an energetic aspect. Temperature has a significant impact on AOB and NOB competition. It has been observed that a high temperature (>30–35 °C) effectively inhibits NOB, due to the faster growth rate of AOB in relation to NOB [50,51]. However, high temperatures are associated with high energy consumption, which greatly reduces process development. In turn, excessively low temperatures (10–15 °C) cause the multiplication of NOB [52], which can develop faster in such conditions than AOB [53]. These dependencies should be balanced. In turn, the optimal temperature for AAOB growth is 30–40 °C [54]. Considering energy consumption, it is recommended that the temperature in the deammonification process is 20–35 °C [15,51]; however, our research reports that it is possible to maintain stable deammonification even at lower temperatures.

Intermittent aeration, however, played an important role in maintaining the process. It has already been tested many times due to the lower costs of aeration compared to continuous aeration systems [55]. It has been found that the application of an appropriate strategy can reduce energy consumption without affecting the course of the process [56].

4. Conclusions

The increase in R due to the extension of the non-aerated phase positively influenced the recovery of the process efficiency under low-temperature conditions in the SBR. The

modeling results confirmed these experimental results, showing a positive effect on the NPR/AUR ratio with the increasing R at low temperatures. A higher temperature dependency on the specific anammox growth rates was found at the lower temperatures θ for 11–17 °C = 1.71 in comparison with the higher temperatures θ for 17–30 °C = 1.12

An excessively high NH_4-N loading rate increased the pool of FA, which is a known inhibitor for anammox bacteria, while low NH_4-N concentrations limit substrate availability and promote the growth of *Nitrosomonas* over AAOB. The high abundance of *Candidatus* Brocadia confirmed that favourable conditions had been selected for the deammonification system to operate under low temperatures. The non-equilibrium state of the experimental system connected to the ordered modifications of the operational conditions emphasized the important role of the disturbances in generating bacterial community diversity. The observed influence of the particular parameters on the microbial diversity was not uniform at the defined parameter value ranges. For instance, in our study, a temperature range from 26 °C to 14 °C was considered an ordering factor, promoting selection of the defined bacterial genera in deammonifiaction systems, especially AOB from the *Ntirosomons* genera. This resulted in a reduction in the biodiversity index values. However, along with the decrease below 12 °C, the temperature's influence on the bacterial community changed and led to disordering effects, which led to community reorganization, as well as promoting general biodiversity. Due to the complexity and ambiguity of the processes taking place in deammonifiaction systems, a combined approach involving technological measurements, microbial analysis and mathematical modeling, proposed in this study, is essential to develop efficient strategies for further system optimization.

Supplementary Materials: The following are available online at https://www.mdpi.com/article/10.3390/en14133961/s1, Figure S1: Changes in composition of the microbial community during experiment at phylum level.

Author Contributions: Conceptualization, H.A.-H.; methodology, H.A.-H., J.M. (Joanna Majtacz) and X.L.; validation, P.K, X.L. and J.M. (Jacek Makinia.); formal analysis, H.A.-H., D.G.; investigation, H.A.-H., D.G., X.L. and J.M. (Joanna Majtacz); writing—original draft preparation, H.A.-H., D.G., X.L., P.K. and J.M. (Joanna Majtacz); writing—review and editing, J.M.; visualization, D.G. and J.M. (Joanna Majtacz); supervision J.M. (Jacek Makinia.) All authors have read and agreed to the published version of the manuscript.

Funding: Founded from the internal sources of the Gdansk University of Technology.

Institutional Review Board Statement: Not applicable.

Informed Consent Statement: Not applicable.

Data Availability Statement: Not applicable.

Acknowledgments: We would like to thank the reviewers for their helpful comments and for improving the manuscript.

Conflicts of Interest: The authors declare no conflict of interest.

References

1. Nawaz, A.; Singh Arora, A.; Mun Yun, C.; Cho, H.; Lee, M. Cost effective nitrogen removal—Novel control strategies. *Int. J. Comput. Methods Exp. Meas.* **2019**, *7*, 376–384. [CrossRef]
2. Klaus, S.; Baumler, R.; Rutherford, B.; Thesing, G.; Zhao, H.; Bott, C. Startup of a Partial Nitritation-Anammox MBBR and the Implementation of pH-Based Aeration Control. *Water Environ. Res.* **2017**, *89*, 500–508. [CrossRef]
3. Lackner, S.; Gilbert, E.M.; Vlaeminck, S.E.; Joss, A.; Horn, H.; van Loosdrecht, M.C.M. Full-scale partial nitritation/anammox experiences—An application survey. *Water Res.* **2014**, *55*, 292–303. [CrossRef]
4. Cao, Y.; Van Loosdrecht, M.C.M.; Daigger, G.T. Mainstream partial nitritation–anammox in municipal wastewater treatment: Status, bottlenecks, and further studies. *Appl. Microbiol. Biotechnol.* **2017**, *101*, 1365–1383. [CrossRef]
5. Trojanowicz, K.; Plaza, E.; Trela, J. Pilot scale studies on nitritation-anammox process for mainstream wastewater at low temperature. *Water Sci. Technol.* **2016**, *73*, 761–768. [CrossRef] [PubMed]
6. Miao, Y.; Peng, Y.; Zhang, L.; Li, B.; Li, X.; Wu, L.; Wang, S. Partial nitrification-anammox (PNA) treating sewage with intermittent aeration mode: Effect of influent C/N ratios. *Chem. Eng. J.* **2018**, *334*, 664–672. [CrossRef]

7. Al-Hazmi, H.; Lu, X.; Majtacz, J.; Kowal, P.; Xie, L.; Makinia, J. Optimization of the aeration strategies in a deammonification sequencing batch reactor for efficient nitrogen removal and mitigation of N_2O production. *Environ. Sci. Technol.* **2021**, *55*, 1218–1230. [CrossRef] [PubMed]
8. Wang, X.; Qi, G.; Yan, Y.; Gao, D. Influence of temperature fluctuations on one-stage deammonification systems in northern cold region. *Environ. Sci. Pollut. Res.* **2018**, *25*, 18632–18641. [CrossRef]
9. Hoekstra, M.; Geilvoet, S.P.; Hendrickx, T.L.G.; van Erp Taalman Kip, C.S.; Kleerebezem, R.; van Loosdrecht, M.C.M. Towards mainstream anammox: Lessons learned from pilot-scale research at WWTP Dokhaven. *Environ. Technol.* **2019**, *40*, 1721–1733. [CrossRef]
10. Hoekstra, M.; de Weerd, F.A.; Kleerebezem, R.; van Loosdrecht, M.C.M. Deterioration of the anammox process at decreasing temperatures and long SRTs. *Environ. Technol.* **2018**, *39*, 1–33. [CrossRef]
11. Li, J.; Bai, L.; Qiang, Z.; Dong, H.; Wang, D. Nitrogen removal through "Candidatus brocadia sinica" treating high-salinity and low-temperature wastewater with glycine addition: Enhanced performance and kinetics. *Bioresour. Technol.* **2018**, *270*, 755–761. [CrossRef] [PubMed]
12. Gilbert, E.M.; Agrawal, S.; Karst, S.M.; Horn, H.; Nielsen, P.H.; Lackner, S. Low temperature partial nitritation/anammox in a moving bed biofilm reactor treating low strength wastewater. *Environ. Sci. Technol.* **2014**, *48*, 8784–8792. [CrossRef] [PubMed]
13. Akaboci, T.R.V.; Gich, F.; Ruscalleda, M.; Balaguer, M.D.; Colprim, J. Assessment of operational conditions towards mainstream partial nitritation-anammox stability at moderate to low temperature: Reactor performance and bacterial community. *Chem. Eng. J.* **2018**, *350*, 192–200. [CrossRef]
14. Lotti, T.; Kleerebezem, R.; van Loosdrecht, M.C.M. Effect of temperature change on anammox activity. *Biotechnol. Bioeng.* **2015**, *112*, 98–103. [CrossRef] [PubMed]
15. Sobotka, D.; Czerwionka, K.; Makinia, J. Influence of temperature on the activity of anammox granular biomass. *Water Sci. Technol.* **2016**, *73*, 2518–2525. [CrossRef]
16. Kaewyai, J.; Noophan, P.L.; Wantawin, C.; Munakata-Marr, J. Recovery of enriched anammox biofilm cultures after storage at cold and room temperatures for 164 days. *Int. Biodeterior. Biodegrad.* **2019**, *137*, 1–7. [CrossRef]
17. Wu, P.; Chen, Y.; Ji, X.; Liu, W.; Lv, G.; Shen, Y.; Zhou, Q. Fast start-up of the cold-anammox process with different inoculums at low temperature (13 °C) in innovative reactor. *Bioresour. Technol.* **2018**, *267*, 696–703. [CrossRef]
18. Ma, B.; Bao, P.; Wei, Y.; Zhu, G.; Yuan, Z.; Peng, Y. Suppressing nitrite-oxidizing bacteria growth to achieve nitrogen removal from domestic wastewater via anammox using intermittent aeration with low dissolved oxygen. *Sci. Rep.* **2015**, *5*, 13048. [CrossRef]
19. Vlaeminck, S.E.; Clippeleir, H.; Verstraete, W. Microbial resource management of one-stage partial nitritation/anammox. *Microb. Biotechnol.* **2012**, *5*, 433–448. [CrossRef] [PubMed]
20. Yang, S.; Xu, S.; Zhou, Y.; Mohammed, A.; Ashbolt, N.J.; Liu, Y. The importance of integrated fixed film activated sludge reactor and intermittent aeration in nitritation-anammox systems: Understanding reactor optimization for lagoon supernatant treatment. *International Biodeterior. Biodegrad.* **2020**, *149*, 104938. [CrossRef]
21. Pereira, A.D.; Fernandes, L.D.A.; Castro, H.M.C.; Leal, C.D.; Carvalho, B.G.P.; Dias, M.F.; Araújo, J.C.D. Nitrogen removal from food waste digestate using partial nitritation-anammox process: Effect of different aeration strategies on performance and microbial community dynamics. *J. Environ. Manag.* **2019**, *251*, 109562. [CrossRef] [PubMed]
22. Miao, Y.; Zhang, L.; Li, B.; Zhang, Q.; Wang, S.; Peng, Y. Enhancing ammonium oxidizing bacteria activity was key to single-stage partial nitrification-anammox system treating low-strength sewage under intermittent aeration condition. *Bioresour. Technol.* **2017**, *231*, 36–44. [CrossRef]
23. Al-Hazmi, H.; Grubba, D.; Majtacz, J.; Kowal, P.; Mąkinia, J. Evaluation of Partial Nitritation/Anammox (PN/A) Process Performance and Microorganisms Community Composition under Different C/N Ratio. *Water* **2019**, *11*, 2270. [CrossRef]
24. Dapena-Mora, A.; Van Hulle, S.W.H.; Campos, J.L.; Méndez, R.; Vanrolleghem, P.A.; Jetten, M. Enrichment of Anammox biomass from municipal activated sludge: Experimental and modeling results. *J. Chem. Technol. Biotechnol.* **2004**, *79*, 1421–1428. [CrossRef]
25. Anthonisen, A.C.; Loehr, R.C.; Prakasam, T.B.S.; Srinath, E.G. Inhibition of nitrification by ammonia and nitrous acid. *J. Water Pollut. Control. Fed.* **1976**, *48*, 835–852.
26. Lu, X.; Pereira, D.S.T.; Al-Hazmi, H.E.; Majtacz, J.; Zhou, Q.; Xie, L.; Makinia, J. Model-Based Evaluation of N2O Production Pathways in the Anammox-Enriched Granular Sludge Cultivated in a Sequencing Batch Reactor. *Environ. Sci. Technol.* **2018**, *52*, 2800–2809. [CrossRef] [PubMed]
27. Vavilin, V.A.; Vasiliev, V.B.; Rytov, S.V.; Ponomarev, A.V. Modeling ammonia and hydrogen sulfide inhibition in anaerobic digestion. *Water Res.* **1995**, *29*, 827–835. [CrossRef]
28. Prigogine, I. Time, Structure, and Fluctuations. *Science* **1978**, *201*, 777–785. [CrossRef]
29. Klindworth, A.; Pruesse, E.; Schweer, T.; Peplies, J.; Quast, C.; Horn, M.; Glöckner, F.O. Evaluation of general 16S ribosomal RNA gene PCR primers for classical and next-generation sequencing-based diversity studies. *Nucleic Acids Res.* **2013**, *41*, e1. [CrossRef] [PubMed]
30. Blankenberg, D.; Gordon, A.; Von Kuster, G.; Coraor, N.; Taylor, J.; Nekrutenko, A.; Team, G. Manipulation of FASTQ data with galaxy. *Bioinformatics* **2010**, *26*, 1783–1785. [CrossRef] [PubMed]
31. Parks, D.H.; Beiko, R.G. Identifying biologically relevant differences between metagenomic communities. *Bioinformatics* **2010**, *26*, 71. [CrossRef] [PubMed]

32. Ali, M.; Okabe, S. Anammox-based technologies for nitrogen removal: Advances in process start-up and remaining issues. *Chemosphere* **2015**, *141*, 144–153. [CrossRef]
33. Lotti, T.; Kleerebezem, R.; Van Erp Taalman Kip, C.; Hendrickx, T.L.G.; Kruit, J.; Hoekstra, M.; Van Loosdrecht, M.C.M. Anammox growth on pretreated municipal wastewater. *Environ. Sci. Technol.* **2014**, *48*, 7874–7880. [CrossRef]
34. Gilbert, E.M.; Agrawal, S.; Schwartz, T.; Horn, H.; Lackner, S. Comparing different reactor configurations for Partial Nitritation/Anammox at low temperatures. *Water Res.* **2015**, *81*, 92–100. [CrossRef]
35. Wells, G.F.; Shi, Y.; Laureni, M.; Rosenthal, A.; Szivák, I.; Weissbrodt, D.G.; Joss, A.; Buergmann, H.; Johnson, D.R.; Morgenroth, E. Comparing the Resistance, Resilience, and Stability of Replicate Moving Bed Biofilm and Suspended Growth Combined Nitritation-Anammox Reactors. *Environ. Sci. Technol.* **2017**, *51*, 5108–5117. [CrossRef]
36. Lackner, S.; Welker, S.; Gilbert, E.M.; Horn, H. Influence of seasonal temperature fluctuations on two different partial nitritation-anammox reactors treating mainstream municipal wastewater. *Water Sci. Technol.* **2015**, *72*, 1358–1363. [CrossRef] [PubMed]
37. Feng, Y.; Lu, X.; Al-Hazmi, H.; Mąkinia, J. An overview of the strategies for the deammonification process start-up and recovery after accidental operational failures. *Rev. Environ. Sci. Biotechnol.* **2017**, *16*, 541–568. [CrossRef]
38. Laureni, M.; Falås, P.; Robin, O.; Wick, A.; Weissbrodt, D.G.; Nielsen, J.L.; Ternes, T.A.; Morgenroth, E.; Joss, A. Mainstream partial nitritation and anammox: Long-term process stability and effluent quality at low temperatures. *Water Res.* **2016**, *101*, 628–639. [CrossRef]
39. Zekker, I.; Rikmann, E.; Mandel, A.; Kroon, K.; Seiman, A.; Mihkelson, J.; Tenno, T.; Tenno, T. Step-wise temperature decreasing cultivates a biofilm with high nitrogen removal rates at 9 °C in short-term anammox biofilm tests. *Environ. Technol.* **2016**, *37*, 1933–1946. [CrossRef] [PubMed]
40. Morales, N.; Val del Río, Á.; Vázquez-Padín, J.R.; Méndez, R.; Campos, J.L.; Mosquera-Corral, A. The granular biomass properties and the acclimation period affect the partial nitritation/anammox process stability at a low temperature and ammonium concentration. *Process. Biochem.* **2016**, *51*, 2134–2142. [CrossRef]
41. Isanta, E.; Reino, C.; Carrera, J.; Pérez, J. Stable partial nitritation for low-strength wastewater at low temperature in an aerobic granular reactor. *Water Res.* **2015**, *80*, 149–158. [CrossRef] [PubMed]
42. Ushiki, N.; Jinno, M.; Fujitani, H.; Suenaga, T.; Terada, A.; Tsuneda, S. Nitrite oxidation kinetics of two Nitrospira strains: The quest for competition and ecological niche differentiation. *J. Biosci. Bioeng.* **2017**, *123*, 581–589. [CrossRef] [PubMed]
43. Lu, X.; Yin, Z.; Sobotka, D.; Wisniewski, K.; Czerwionka, K.; Xie, L.; Zhou, Q.; Makinia, J. Modeling the pH effects on nitrogen removal in the anammox-enriched granular sludge. *Water Sci. Technol.* **2017**, *75*, 378–386. [CrossRef] [PubMed]
44. Sobotka, D.; Zhai, J.; Makinia, J. Generalized temperature dependence model for anammox process kinetics. *Sci. Total Environ.* **2021**, *775*, 145760. [CrossRef]
45. Kwak, W.; Rout, P.R.; Lee, E.; Bae, J. Influence of hydraulic retention time and temperature on the performance of an anaerobic ammonium oxidation fluidized bed membrane bioreactor for low-strength ammonia wastewater treatment. *Chem. Eng. J.* **2020**, *386*, 123992. [CrossRef]
46. Gude, V.G. Energy and water autarky of wastewater treatment and power generation systems. *Renew. Sustain. Energy Rev.* **2015**, *45*, 52–68. [CrossRef]
47. Hendrickx, T.L.; Wang, Y.; Kampman, C.; Zeeman, G.; Temmink, H.; Buisman, C.J. Autotrophic nitrogen removal from low strength waste water at low temperature. *Water Res.* **2012**, *46*, 2187–2193. [CrossRef]
48. Hu, B.L.; Zheng, P.; Tang, C.J.; Chen, J.W.; van der Biezen, E.; Zhang, L.; Ni, B.J.; Jetten, M.S.; Yan, J.; Yu, H.Q.; et al. Identification and quantification of anammox bacteria in eight nitrogen removal reactors. *Water Res.* **2010**, *44*, 5014–5020. [CrossRef]
49. Kartal, B.; Tan, N.C.; Van de Biezen, E.; De Kampschreur, M.J.; Van Loosdrecht, M.C.; Jetten, M.S. Effect of nitric oxide on anammox bacteria. *Appl. Environ. Microbiol.* **2010**, *76*, 6304–6306. [CrossRef]
50. Kanders, L.; Areskoug, T.; Schneider, Y.; Ling, D.; Punzi, M.; Beier, M. Impact of seeding on the start-up of one-stage deammonification MBBRs. *Environ. Technol.* **2014**, *35*, 2767–2773. [CrossRef]
51. Guo, J.; Peng, Y.; Huang, H.; Wang, S.; Ge, S.; Zhang, J.; Wang, Z. Short- and long-term effects of temperature on partial nitrification in a sequencing batch reactor treating domestic wastewater. *J. Hazard. Mater.* **2010**, *179*, 471–479. [CrossRef] [PubMed]
52. Kouba, V.; Vejmelkova, D.; Proksova, E.; Wiesinger, H.; Concha, M.; Dolejs, P.; Hejnic, J.; Jenicek, P.; Bartacek, J. High-Rate Partial Nitritation of Municipal Wastewater after Psychrophilic Anaerobic Pretreatment. *Environ. Sci. Technol.* **2017**, *51*, 11029–11038. [CrossRef] [PubMed]
53. Hellinga, C.; Schellen, A.A.; Mulder, J.W.; Vanloosdrecht, M.C.; Heijnen, J.J. The sharon process: An innovative method for nitrogen removal from ammonium-rich waste water. *Water Sci. Technol.* **1998**, *37*, 135–142. [CrossRef]
54. Strous, M.; Kuenen, J.G.; Jetten, M.S. Key physiology of anaerobic ammonium oxidation. *Appl. Environ. Microbiol.* **1999**, *65*, 3248–3250. [CrossRef] [PubMed]
55. Vázquez-Padín, J.R.; Pozo, M.J.; Jarpa, M.; Figueroa, M.; Franco, A.; Mosquera-Corral, A.; Campos, J.L.; Méndez, R. Treatment of anaerobic sludge digester effluents by the CANON process in an air pulsing SBR. *J Hazard Mater.* **2009**, *166*, 336–341. [CrossRef] [PubMed]
56. Żubrowska-Sudol, M.; Yang, J.; Trela, J.; Plaza, E. Evaluation of deammonification process performance at different aeration strategies. *Water Sci. Technol.* **2011**, *63*, 1168–1176. [CrossRef] [PubMed]